# Investigation of optical properties of Er3+-doped Ga1As39S60 glasses quenched in salt batch media

**mohammad rezvani** ( m_rezvani@tabrizu.ac.ir )
University of Tabriz https://orcid.org/0000-0002-8250-1460

**Amin Yousefi Dizaj**
University of Tabriz

**Pouya Ahmadi**
University of Tabriz

**Research Article**

**Keywords:** Ga-As-S glasses, Er-doped glasses, optical properties

**Posted Date:** March 1st, 2022

**DOI:** https://doi.org/10.21203/rs.3.rs-843684/v1

# Investigation of optical properties of $Er^{3+}$-doped $Ga_1As_{39}S_{60}$ glasses quenched in salt batch media

**Mohammad Rezvani[1*,b], Amin Yousefi Dizaj[1,a] ,Saideh ahmadpour[1,c], Pouya Ahmadi[1,d]**

*Corresponding Author Email: m_rezvani@tabrizu.ac.ir

1-Department of Material Engineering, University of Tabriz, Tabriz, East Azerbaijan, Iran

## Abstract:

$Er^{3+}$ - doped (0.5-2%wt) $Ga_1As_{39}S_{60}$ glasses were synthesized by melting appropriate amounts of Ga, As, S as starting materials in rotating furnace and consequently quenching in salt batch media ($NaNO_3$ + $KNO_3$) with the temperature of 130℃. X-ray diffraction spectra and FESEM micrograph showed the amorphous nature and homogeneous structure of the prepared samples with no clusters. The glass transition temperature of samples was increased from 183℃ to 206℃ by increasing $Er^{3+}$ amount from 0.5 to 2%wt. The effects of $Er^{3+}$ on absorption coefficient($\alpha$), Fermi energy level($E_F$), direct and indirect forbidden bands, and Urbach energy were investigated and later ones were increased from 1.75 to 1.77ev, from 1.80 to 1.84 ev, from 2.05 to 2.08 ev and from 0.10 to 0.11 ev, respectively with increasing $Er^{3+}$ ions (0.5-2%wt) which confirmed the modifying role of $Er^{3+}$ ions in Ga-As-S system.

*Keywords: Ga-As-S glasses, Er-doped glasses, optical properties*

## Introduction:

Chalcogenide glasses are based on chalcogen elements S, Se, and Te [1]–[3]. These glasses are used as amorphous semiconductors in phase-change memories [4], solar cells [5], sensors [6], and photonics [7]. These glasses are formed by covalence

bonding with network formers such as As, Ge, Sb, Ga, Si or, P, etc [8]. Because of a wide range of glass-forming systems and good crystallization resistance, they possess unique optical properties such as nonlinearity, photosensitivity, and infrared transparency besides low phonon energy, which all of these properties can be optimized for photonic applications [7].

Chalcogenide glasses can also be doped by rare-earth elements, such as Er, Nd, Pr, etc [9]–[11]. The possibility of improvement and altering the properties of these chalcogenide glasses cause these materials to be eligible for numerous applications of crucial optical devices [12]. These glasses are optically highly non-linear and could, therefore, be useful for all-optical switching(AOS) [13]. Because of the sensitivity of the chalcogenide glasses toward absorbing electromagnetic radiations, these glasses exhibit a variety of photoinduced effects as a result of illumination. Different modelings are offered to explain such effects, which can result in the fabrication of diffractive, waveguide, and fiber structures [12].

Achieving information about different optical properties of Chalcogenide glasses is a crucial step in utilizing these materials in applications such as photovoltaic [14], optoelectronics [15], electrochromic performance [16], sensors [6], display devices [17], solar cell [5], and photo-electrochemistry [18]. The optical properties of materials depend on various parameters like preparation methods and techniques, the preparatory conditions, surface morphology, also dopants, and interaction with the surrounding environment. One of the important optical properties of glasses is the optical absorption coefficient. Studying the spectral behavior of the absorption coefficient in semiconducting materials gives us crucial knowledge about the electronic state in the high energy regions of the optical absorption spectrum. The other lower energy part of the spectrum is related to the atomic vibrations [19], [20].

The Beer-Lambert law is one of the Optic's principal laws that relates the attenuation of light to the properties of the material through which the light is traveling. This law is generally written in such a manner:

$$\mathrm{I} = I_0 e^{-\alpha bc}$$

That I and $I_0$ is the intensity of light before and after passing through the material, respectively. $\alpha$ is absorption coefficient dependent on wavelength, b is the thickness, and c is the concentration of material [21].

This famous law is generally expressed in this way for transparent materials :

$$I = I_0 e^{-\alpha d} \quad (1)$$

As a result, the absorption coefficient for transparent glasses can be calculated when the transmittance and thickness values are available [14].

In addition to the optical absorption coefficient, the Fermi energy level, direct and indirect forbidden bands, and Urbach energy are crucial to calculate [22].

The Fermi energy level is determined by calculating the extinction coefficient that obeys Fermi-Dirac Equation [23] :

$$K = \frac{1}{1 + exp[\,(E_F - E)/K_B T]} \quad (2)$$

That $E_F$ is Fermi energy level, $K_B$ Boltzmann constant, T is Absolute Temperature, E is incident photons energy, and K is the extinction coefficient.

On the other hand, Photon energy and the extinction coefficient can be calculated by the following equations:

$$E = \frac{hc}{\lambda} \quad (3)$$

$$K = \frac{\alpha\lambda}{4\pi} \quad (4)$$

That c is the speed of light, h is Plank's constant, λ is the incident wavelength, and $\alpha$ is absorption coefficient [23].

By using these equations, we can calculate the Fermi energy level that is applied in determining the electrical and thermal characteristics of the glasses[24].

The correspondence between the absorption coefficient ($\alpha$) and the incident photon energy (hν) can be determined by using Tauc's relationship in the high absorption region of semiconductor, as follows [25]–[27]:

$$ahv = a_0\,(\,hv - E_g\,)^n \quad (5)$$

where $a_0$ is a constant and also named the band tailing parameter which is independent of energy, and $E_g$ Is the optical energy gap, which is established between the localized states close to the mobility edges as stated by the density of states model suggested by Mott and Davis [27]–[29].
In Eq.(4) there is another constant (n), which is called the power factor of the transition mode. This constant is because of the nature of the material. It varies from one to another, whether it is crystalline or amorphous, and it is also dependent on the photon transition. The values of (n) for direct allowed, Indirect allowed, direct forbidden and indirect forbidden transitions are $\frac{1}{2}, 2, \frac{3}{2}, 3$, respectively [26], [29].

Finally, with the plotting of $(ah\upsilon)^{\frac{1}{n}}$ against the energy of the photons ( in other words drawing Tauc plot ) and dividing the y-intercept by slope of the linear section of the plotted diagrams, we can calculate the energy band gap of optical transitions [23], [30].

As the final essential properties to measure in glasses, we will discuss Urbach Energy.

Urbach's experimental law is given by the following equation [23].

$$\alpha = \beta \exp(\frac{hv}{E_U}) \tag{6}$$

Where $\beta$ is constant and $E_U$ denotes the energy of the band tail or sometimes called Urbach energy.

Taking the logarithm of the two sides of the last equation, hence one can get a straight line equation. It is given as follows:

$$\mathrm{Ln}(\alpha) = Ln\beta + \frac{hv}{E_U} \tag{7}$$

Eventually, with plotting $Ln(a)$ against incident photon energy $hv$ and reversing the slope of the plotted diagram, Urbach energy is calculated[14].

## Experimental

In this study, we investigated the effect of adding 0.5-2%wt $Er^{3+}$to the optical properties of $Ga_1As_{39}S_{60}$glasses. The glasses were synthesized by melting optimal amounts of highly pure As (Sigma Aldrich, 99.999% Purity), Ga(Sigma Aldrich, 99.999% Purity), S ( Sigma Aldrich, 99.99% Purity) and the $Er_2S_3$ (PubChem, 99.999% Purity). The glasses' compositions, and their codes are summarized in Table1.

Table 1. The glasses' compositions and their codes.

| Glass composition | Specimen code |
|---|---|
| $Ga_1As_{39}S_{60}$- 0.5%wt Er | G-0.5%Er |
| $Ga_1As_{39}S_{60}$- 1%wt Er | G-1%Er |
| $Ga_1As_{39}S_{60}$- 2%wt Er | G-2%Er |

All the raw materials were weighted in the glove box with a precision of 0.0001 gr and then trilled into silica ampoules that were pre-cleaned by soaking in HF acid, distilled water, and acetone, respectively, following heat-treating in a furnace with the temperature of $700°C$ for 2 hours. The open ends of the ampoules were sealed by a vacuum pump under $10^{-3}$ Torr pressure for 3 minutes with an acetylene torch simultaneously. The ampoules were placed in the rocking furnace, melted at $650°C$ , and kept for 8 h to obtain homogenized melting and subsequently quenched in a salt-bath ($NaNO_3 + KNO_3$) at $130°C$. The obtained glasses were annealed at $160°C$ for 2 h to remove the remaining thermal stress. For further analysis, glass samples were cut into disks with 3 mm thickness and then polished.

The X-ray diffraction (XRD) patterns of the powdered samples obtained by Philips X-pert-MDD system were used to check the produced specimen's amorphous nature. The X-ray pattern was obtained by Cu source emitting 0.15406 nm radiation (30kV, step size: $0.02°C$, time per step: 1.2S). The structure and the composition of the glasses were checked by field emission scanning electron microscope (MIRA3TESCAN-XMU) equipped with an energy dispersive X-ray spectroscopy(EDXS) detector. The UV-vis spectra of the glasses were also measured by UV-Vis-NIR Shimadzu 3100 to study transparency, determine absorption and extinction coefficients, and investigate direct and indirect bandgap, Fermi energy, and Urbach energy of the glasses. For having smooth and parallel

surfaces of the specimens required for UV-Vis-NIR analyses, polishing was done on the specimens. The glass transition temperature ($T_g$) was measured by DSC60-Shimadzu differential scanning calorimeter using a heating rate of 10 $\frac{℃}{min}$.

## Result and discussion

Figure 1 shows the XRD patterns of G-(0.5-2%) Er glasses. All of the patterns have two broad bands without any sharp peaks associated with crystalline phases, which confirms the amorphous structure of the prepared samples. We can assume that two broad bands in the XRD pattern are related to nucleants that may grow slightly through heat treatment at crystallization temperature.

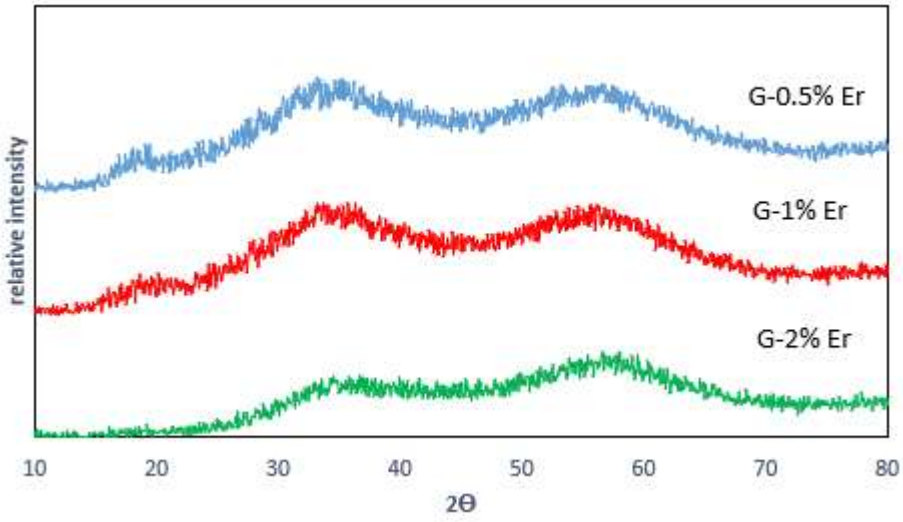


Fig 1. XRD Pattern of G-(0.5-2%) Er glasses.

FESEM micrograph of the G-2%Er glass (the glass with maximum concentrartion of $Er^{3+}$ ions among the three investigated compositions) and it's EDXS spectra were presented in the Figure (2.a) and (2.b) respectively. As it shown, there was no Er-rich clusters in the glass structure which means that the Er ions were solved homogenously in the glass structure.

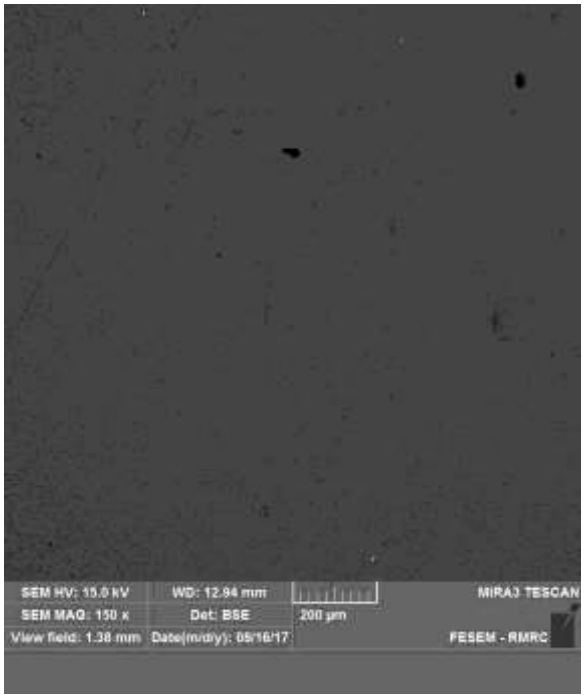


(2.a)

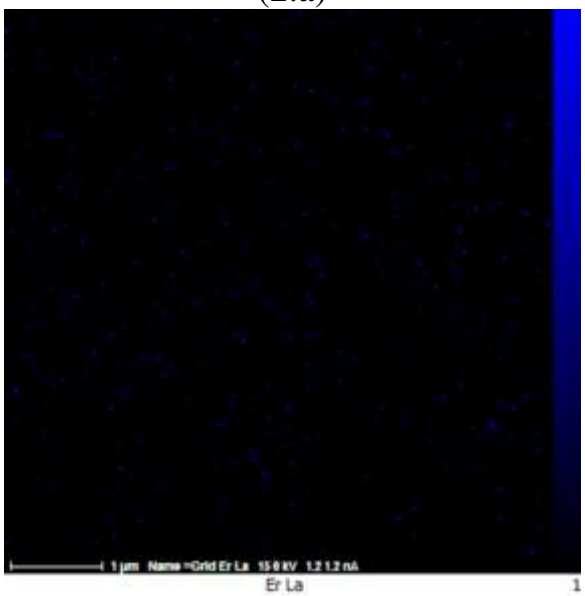


(2.b)

Fig.2. (a) FESEM micrograph of the G-2%Er glass and (b) it's EDXS spectra.

Figure 3 shows DSC spectra of G-(0.5-2%) Er glasses. The glass transition temperature usually is effected by bonding strength and mean coordination number. Glasses with higher mean coordination number and bonding strength will have elevated glass transition temperature. By introducing $Er^{3+}$ ions to Ga-As-S glass system, the mean coordination number will be decreased because of higher radius of

Er ions ($\sim 226ppm$) in comparison with Ga ($\sim 135pm$), $As$ ($\sim 114pm$) and $S$ ($\sim 88pm$) elements. On the other hand, the melting point and bonding strength of $Er_2S_3$ ($\sim 1730℃$) are higher than Ga-As-S system ($\sim 300℃$). As it shown in Figure 3, the glass transition temperature was increased from 183 ℃ to 206℃ by increasing Er amount from 0.5 to 2%wt which means that the latter factor is more effective than first one and causes the increase in the glass transition temperature.

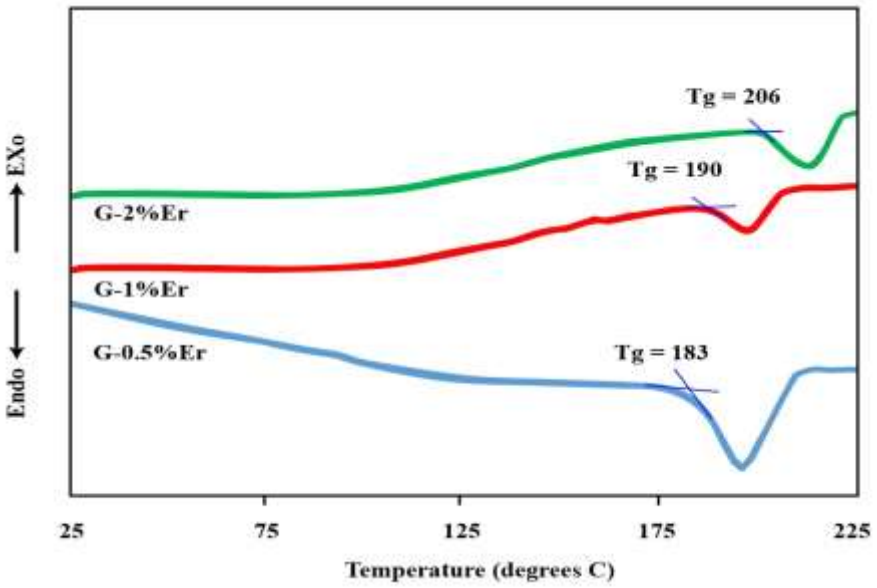


Fig 3. DSC Pattern of G-(0.5-2%) Er glasses.

In order to study absorption and extinction coefficients of G-(0.5-2%) Er glasses, UV-Visible spectra of them were investigated. In figure (4.a), UV-Visible spectra of the samples are shown. The transmittance of the glasses is so close that it is not easy to distinguish them from each other. To compare the transmittance of the prepared samples in the visible and near-IR region, the range of wavelength in the figure.4 (a) (200-1200 nm) was reduced to 570-770 nm in figure.4 (b). It can be seen that with an increase in Er amount in the glass compositions, the transmittance in the visible region was increased. Instead, after passing the visible region, the absorption mechanism was changed. Thus, samples with higher amounts of Er had the lowest transmittance, and samples with lower amounts of Er had the highest transmittance.

In our previous study [31], We have talked about the low solubility of Er ions in $As_2S_3$ Glasses. There were no peaks observed associating with 4f-4f transitions of Er ions in the mentioned study. When Ga was added to $As_2S_3$ Glasses, as a modifier, modified the glass structure to a non-compress structure and increased the solubility of Er ions. Hence, in figure (4.a), we can see the peaks associating with 4f-4f

transitions of Er ions. The role of Ga as a modifier was confirmed in the previous studies [32], in which, the increase in the amount of $Ga$ in the composition causes open and non-compress structure and increases the phonon energy, leading to a decrease in the transmittance. The decreased transmittance in the IR region [32] and the presence of 4f-4f transitions of Er ions in Uv-Visible spectra confirms(present study) the role of Ga as modifier more than before.

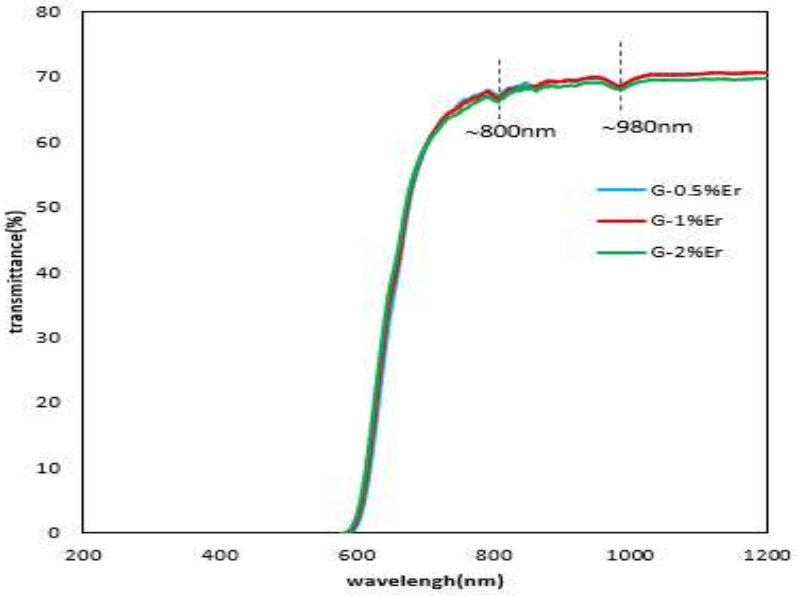


(a)

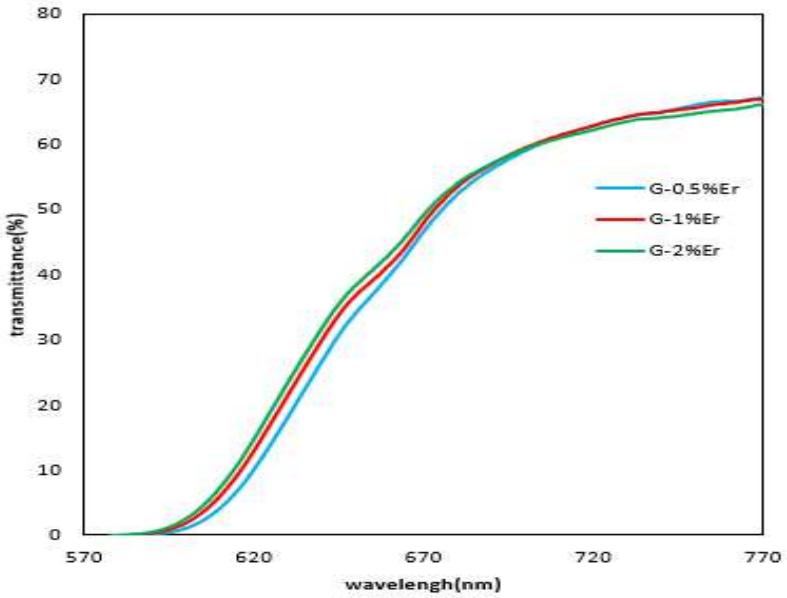


(b)

Fig. 4.(a) UV-Visible spectra of G-(0.5-2%) Er glasses, (b) Transmittance spetra of G-(0.5-2%) Er glasses in range of 570-770 nm.

The absorption coefficient of the samples (2.1cm thickness) was calculated using the Beer-Lambert equation. As shown in the figure.5 (a), with an increase in the amount of Er in samples, the absorption coefficient was decreased in the visible region. The difference between the values of the absorption coefficients for different samples is insignificant. Thus, it is not easy to separate the UV-Visible spectra of each sample with different amounts of Er. We have reduced the wavelength the range to 570-770 nm in the figure. 5 (b) to solve this issue.

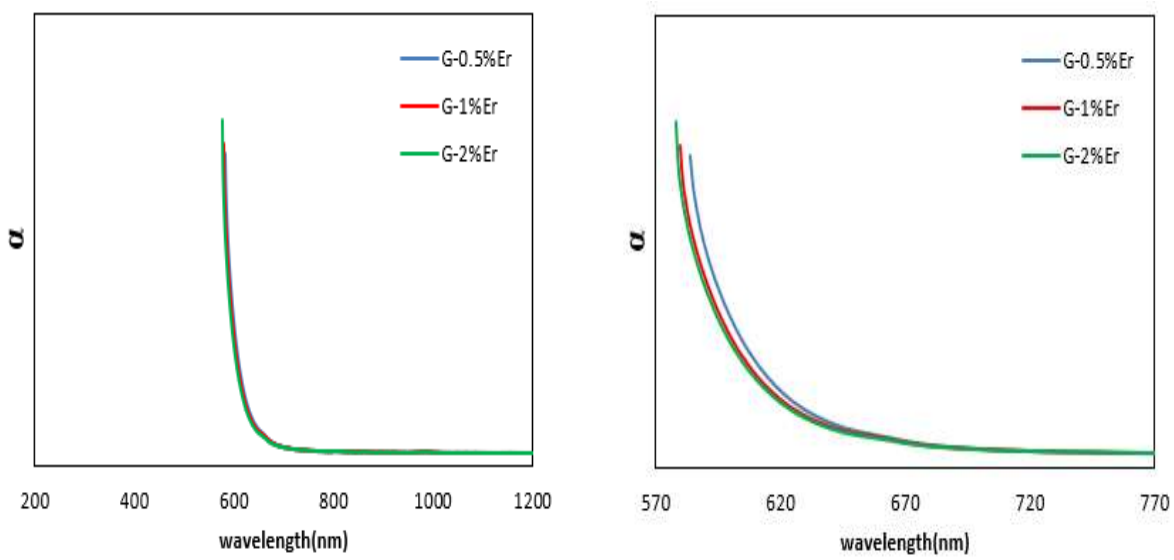


Fig.5. **(a)** Absorption coefficient to wavelength figures G-(0.5-2%) Er glasses In UV-Visible range, **(b)** Absorption coefficient to wavelength figures of G-(0.5-2%) Er glasses In range of 570-770 nm.

If the absorbance in the UV region is more than the visible region, the extinction coefficient will obey the Fermi-Dirac distribution equation. Thus, by calculating the extinction coefficient in different wavelengths and plotting the extinction coefficient to incident photons energy (hv) figure, we can calculate the Fermi energy level. Figure (6) shows the extinction coefficient versus the incident photon's energy. Values calculated for the Fermi energy level are brought in Table (2). We can see that with an increase in Er amount, the Fermi energy level increases. This phenomenon can be related to the narrowing of the conduction band. In other words, by increasing the Er amount, semiconductivity reduces, and samples tend to be insulators.

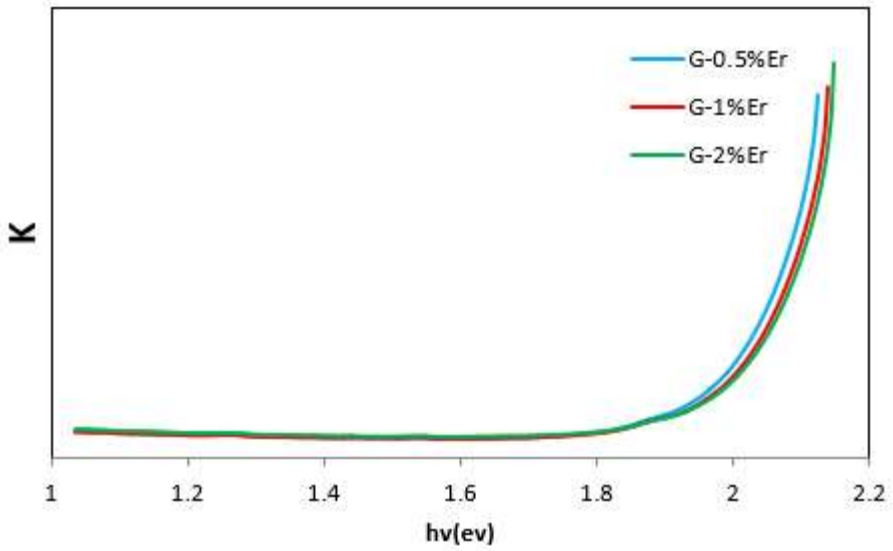


Fig. 6. extinction coefficient to wavelength figures of G-(0.5-2%) Er glasses.

Generally, the forbidden band is the difference between the highest energy level of the valance band and the lowest energy level of the conduction band. This energy difference is equal to the energy required for an electron to leave the outer layer of the atom. Thus the released electron can easily flow inside the solid material as a charged particle. Hence the forbidden band is an essential factor in determining electrical conduction in solid materials. In semiconducting materials, there are two kinds of forbidden bands, direct and indirect. Materials in which the highest energy level of the valance band and the lowest energy level of the conduction band have an equal wave vector $\vec{K}$ are materials with a direct forbidden band. In such materials during electron transmission, wave and displacement vectors remain constant, and direct band transmission occurs. On the other hand, there are materials in which the indirect band transmission occurs. In this way, although a photon can only absorb subtle energies, it is capable of taking a significantly massive displacement compared to an electron. Thus the extra amount of displacement is added to the lattice or absorbed from the lattice. Indirect band transmissions have a crucial role in semiconducting materials [25]. To investigate the values of direct and indirect forbidden bands, We drew the Tauc plots of each sample. The direct and indirect forbidden band is measurable by plotting $(\alpha hv)^2$ and $(\alpha hv)^{\frac{1}{2}}$ respectively versus incident photon's energy and attaining the division of the y-intercept to the slope of the linear section of plotted figures. Figure. 7 and 8 show the Tauc plots of G-(0.5-2%) Er glasses for calculating direct and indirect forbidden bands.

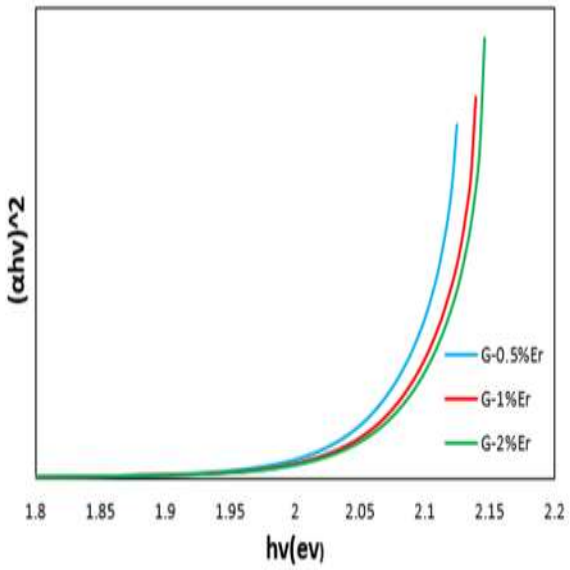

Fig. 7. Tauc Plots G-(0.5-2%) Er glasses (direct forbidden bands).

It was approved before, glasses in which dopants have the role of glass formers in their structure, semiconductive properties will be increased with increasing dopants; thus, the forbidden bands of the glasses will be decreased. As claimed in our previous studies [32], Er has appeared as a modifier to the structure of $Ga_1As_{39}S_{60}$ glasses. Hence, it was anticipated that Er ions as modifiers would decrease the semiconductive properties in contrast with the glass formers dopants. Calculated values for the optical properties of G-(0.5-2%) Er glasses are brought in Table (2); as we anticipated, with increasing Er, values for direct and indirect forbidden bands were increased. The increase in values of direct and indirect forbidden bands and Fermi energy level confirms the role of Er as a modifier which was claimed before[32].

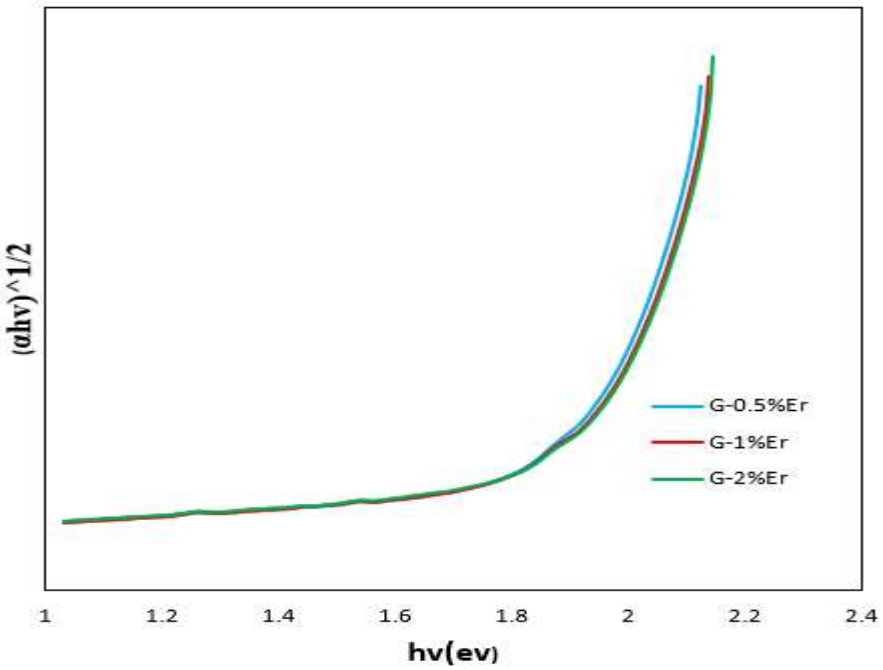

Fig.8. Tauc plots of G-(0.5-2%) Er glasses (indirect forbidden band).

Table 2: Optical calculated values for G-(0.5-2%) Er glasses glasses glasses

| Sample code | $E_F$(ev) | $E_{indirect}$(ev) | $E_{direct}$(ev) | $E_U$(ev) |
|---|---|---|---|---|
| G-0.5%Er | 1.75 | 1.80 | 2.05 | 0.10 |
| G-1%Er | 1.76 | 1.83 | 2.07 | 0.11 |
| G-2%Er | 1.77 | 1.84 | 2.08 | 0.11 |

Furthermore, as the last optical calculation, we investigated the Urbach energy. The optical absorption spectra of semiconducting materials provide the primary information about its composition, and its optical band gap hence has particular importance. The optical absorption spectra of the semiconductor can be categorized into three main regions; (1) weak absorption region, which appear from defects and impurities, (2) absorption edge region, which appear due to perturbation of structural and disorder of the system and (3) the region of strong absorption that determines the optical energy gap. There is an exponential region called Urbach tail Beside the absorption coefficient curve and close to the optical band edge. This exponential tail arises in the low crystalline, poor crystalline, disordered, and amorphous materials because these materials have localized states which extended in the bandgap [33]–[35].

Indeed, in perfect semiconducting crystals, there is a precise forbidden band between the valance and the conduction bands. However, in amorphous semiconductors, the extension of the valance and the conduction bands end abruptly in the edge regions of the bands, thus creating band tails in the forbidden band region that these tails and localized regions are regarding Urbach band tails [36]. Nevertheless, sometimes even some defects and pollutants present in amorphous materials can cause these localized regions in the forbidden band, as well [14] .Figure 9 shows the plots of $Ln(\alpha)$ versus $hv$ for each sample. We can obtain the Urbach energy by calculating the slope of the mentioned figures. The calculated values are brought in Table (2). The Urbach energy of the samples is increased slightly with increasing Er. Since Urbach energy has an inverse relationship with structural order, we can see that, with increasing Er, the Urbach energy of the samples is increased; thus, the structural disorder of the samples increases which confirms the modifying role of Er ions.

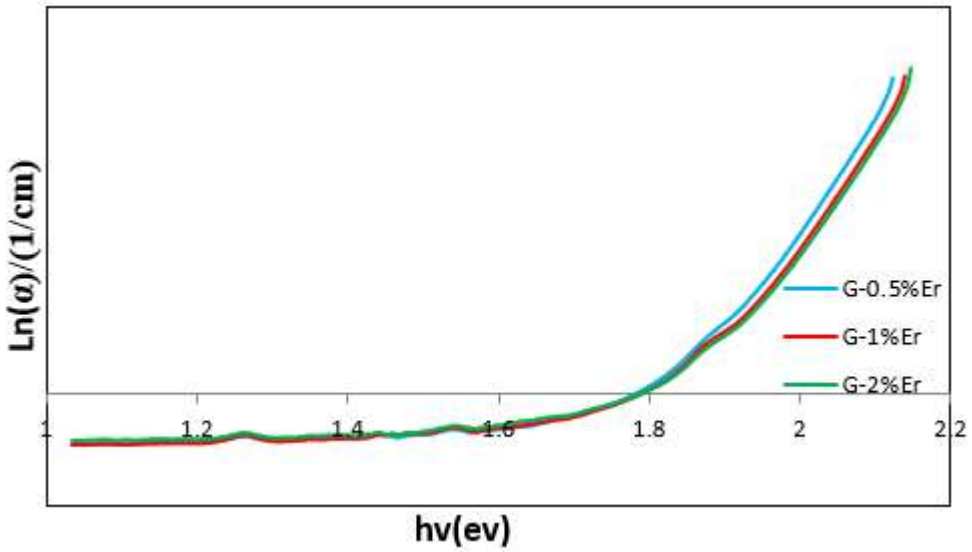


Fig.9. Ln(α) versus hv plots of G-(0.5-2%) Er glasses.

**Conclusion**:

It was presented that with increasing $Er^{3+}$ (0.5-2%wt) the amorphous nature of $Ga_1As_{39}S_{60}$ glasses was not changed and there was no crystallization in the samples.

For the investigation of Optical properties of the prepared samples, Uv-Vis spectra of samples were prepared. With increasing $Er^{3+}$ ions the transmittance of samples was increased in the visible region and decreased in the IR region, slightly. absorption coefficient($\alpha$), Fermi energy level($E_F$), direct and indirect forbidden bands, and Urbach energy were calculated using Uv-Vis Spectra and relating

equations that were reported before. It was shown that with increasing $Er^{3+}$ ions the order of the glass system decreased due to modifying role of Er and Fermi energy level($E_F$), direct and indirect forbidden bands and Urbach energy was increased from 1.75 to 1.77ev, from 1.80 to 1.84 ev, from 2.05 to 2.08 ev and from 0.10 to 0.11 ev, respectively with increasing $Er^{3+}$ ions (0.5-2%wt).

References:


[1] A. R. Hilton, "Optical properties of chalcogenide glasses," *J. Non-Cryst. Solids*, vol. 2, pp. 28–39, Jan. 1970, doi: 10.1016/0022-3093(70)90118-3.

[2] S. Ahmadpour, M. Rezvani, and P. Bavafa, "The effect of Sn on the physical and optical properties of (Se0.6As0.1Ge0.3)100-xSnx glasses," *Spectrochim. Acta. A. Mol. Biomol. Spectrosc.*, vol. 205, pp. 258–263, Dec. 2018, doi: 10.1016/j.saa.2018.07.027.

[3] M. Ghayebloo, M. Rezvani, and M. Tavoosi, "The relationship between structural and optical properties of Se-Ge-As glasses," *Infrared Phys. Technol.*, vol. 90, pp. 40–47, May 2018, doi: 10.1016/j.infrared.2018.02.004.

[4] M. Nardone, M. Simon, I. V. Karpov, and V. G. Karpov, "Electrical conduction in chalcogenide glasses of phase change memory," *J. Appl. Phys.*, vol. 112, no. 7, p. 071101, Oct. 2012, doi: 10.1063/1.4738746.

[5] K. Singh, N. S. Saxena, O. N. Srivastava, D. Patidar, and T. P. Sharma, "ENERGY BAND GAP OF Se100-XInX CHALCOGENIDE GLASSES," p. 4.

[6] Yu. G. Mourzina *et al.*, "Copper, cadmium and thallium thin film sensors based on chalcogenide glasses," *Anal. Chim. Acta*, vol. 433, no. 1, pp. 103–110, Apr. 2001, doi: 10.1016/S0003-2670(00)01384-2.

[7] B. J. Eggleton, B. Luther-Davies, and K. Richardson, "Chalcogenide photonics," *Nat. Photonics*, vol. 5, no. 3, Art. no. 3, Mar. 2011, doi: 10.1038/nphoton.2011.309.

[8] R. Kerner and M. Micoulaut, "On the glass transition temperature in covalent glasses," *J. Non-Cryst. Solids*, vol. 210, no. 2, pp. 298–305, Mar. 1997, doi: 10.1016/S0022-3093(96)00678-3.

[9] P. V. D. Santos, M. T. D. Araujo, A. S. Gouveia-Neto, J. A. M. Neto, and A. S. B. Sombra, "Optical thermometry through infrared excited upconversion

fluorescence emission in Er/sup 3+/- and Er/sup 3+/-Yb/sup 3+/-doped chalcogenide glasses," *IEEE J. Quantum Electron.*, vol. 35, no. 3, pp. 395–399, Mar. 1999, doi: 10.1109/3.748846.

[10] D. Lezal, J. Pedlikova, and J. Zavadil, "Chalcogenide glasses for optical and photonics applications," *J. Optoelectron. Adv. Mater.*, vol. 6, pp. 133–137, Apr. 2004.

[11] M. F. Churbanov *et al.*, "Chalcogenide glasses doped with Tb, Dy and Pr ions," *J. Non-Cryst. Solids*, vol. 326–327, pp. 301–305, Oct. 2003, doi: 10.1016/S0022-3093(03)00417-4.

[12] A. Zakery and S. R. Elliott, "Optical properties and applications of chalcogenide glasses: a review," *J. Non-Cryst. Solids*, vol. 330, no. 1, pp. 1–12, Nov. 2003, doi: 10.1016/j.jnoncrysol.2003.08.064.

[13] K. Ogusu, J. Yamasaki, S. Maeda, M. Kitao, and M. Minakata, "Linear and nonlinear optical properties of Ag–As–Se chalcogenide glasses for all-optical switching," *Opt. Lett.*, vol. 29, no. 3, pp. 265–267, Feb. 2004, doi: 10.1364/OL.29.000265.

[14] J. Singh, *Optical Properties of Condensed Matter and Applications*. John Wiley & Sons, 2006.

[15] N. Mehta, "Applications of chalcogenide glasses in electronics and optoelectronics: A review," *JSIR Vol6510 Oct. 2006*, Oct. 2006, Accessed: Feb. 28, 2021. [Online]. Available: http://nopr.niscair.res.in/handle/123456789/4967

[16] *Electrochromic Adaptive Infrared Camouflage*. Defense Technical Information Center, 2005.

[17] A. S. Hassanien and A. A. Akl, "Effect of Se addition on optical and electrical properties of chalcogenide CdSSe thin films," *Superlattices Microstruct.*, vol. 89, pp. 153–169, Jan. 2016, doi: 10.1016/j.spmi.2015.10.044.

[18] G. D. Fong, "Photoelectrodes for photoelectrochemical cell devices," US4658087A, Apr. 14, 1987 Accessed: Feb. 28, 2021. [Online]. Available: https://patents.google.com/patent/US4658087/en

[19] F. Urbach, "The Long-Wavelength Edge of Photographic Sensitivity and of the Electronic Absorption of Solids," *Phys. Rev.*, vol. 92, no. 5, pp. 1324–1324, Dec. 1953, doi: 10.1103/PhysRev.92.1324.

[20] M. El-Hagary, M. Emam-Ismail, E. R. Shaaban, and A. El-Taher, "Effect of γ-irradiation exposure on optical properties of chalcogenide glasses Se70S30−xSbx thin films," *Radiat. Phys. Chem.*, vol. 81, no. 10, pp. 1572–1577, Oct. 2012, doi: 10.1016/j.radphyschem.2012.05.012.

[21] D. A. Skoog, F. J. Holler, and S. R. Crouch, *Principles of Instrumental Analysis*, 6th edition. Belmont, CA: Cengage Learning, 2006.

[22] S. G. Bishop, D. A. Turnbull, and B. G. Aitken, "Excitation of rare earth emission in chalcogenide glasses by broadband Urbach edge absorption," *J. Non-Cryst. Solids*, vol. 266–269, pp. 876–883, May 2000, doi: 10.1016/S0022-3093(99)00859-5.
[23] M. S. Shakeri and M. Rezvani, "Optical band gap and spectroscopic study of lithium alumino silicate glass containing Y3+ ions," *Spectrochim. Acta. A. Mol. Biomol. Spectrosc.*, vol. 79, no. 5, pp. 1920–1925, Sep. 2011, doi: 10.1016/j.saa.2011.05.090.
[24] M. S. Shakeri and M. Rezvani, "Optical properties and structural evaluation of Li2O–Al2O3–SiO2–TiO2 glassy semiconductor containing passive agent CeO2," *Spectrochim. Acta. A. Mol. Biomol. Spectrosc.*, vol. 83, no. 1, pp. 592–597, Dec. 2011, doi: 10.1016/j.saa.2011.09.009.
[25] J. Tauc, "Optical Properties of Amorphous Semiconductors," in *Amorphous and Liquid Semiconductors*, J. Tauc, Ed. Boston, MA: Springer US, 1974, pp. 159–220. doi: 10.1007/978-1-4615-8705-7_4.
[26] J. Tauc, *Amorphous and Liquid Semiconductors*. Springer Science & Business Media, 2012.
[27] A. A. Yadav and E. U. Masumdar, "Preparation and characterization of indium doped CdS0.2Se0.8 thin films by spray pyrolysis," *Mater. Res. Bull.*, vol. 45, no. 10, pp. 1455–1459, Oct. 2010, doi: 10.1016/j.materresbull.2010.06.034.
[28] N. F. Mott and E. A. Davis, *Electronic Processes in Non-Crystalline Materials*. Oxford, New York: Oxford University Press, 2012.
[29] K. A. Aly, A. M. Abd Elnaeim, N. Afify, and A. M. Abousehly, "Improvement of the electrical properties of Se3Te1 thin films by In additions," *J. Non-Cryst. Solids*, vol. 358, no. 20, pp. 2759–2763, Oct. 2012, doi: 10.1016/j.jnoncrysol.2012.06.029.
[30] S. John, C. Soukoulis, M. H. Cohen, and E. N. Economou, "Theory of Electron Band Tails and the Urbach Optical-Absorption Edge," *Phys. Rev. Lett.*, vol. 57, no. 14, pp. 1777–1780, Oct. 1986, doi: 10.1103/PhysRevLett.57.1777.
[31] M. Rezvani, A. Yousefi Dizaj, A. Rahimian, and T. Joudi, "The effect of Er on optical and mechanical properties of As2S3 glasses quenched in different media," *Eur. Phys. J. Plus*, vol. 135, p. 532, Jun. 2020, doi: 10.1140/epjp/s13360-020-00502-9.
[32] A. Y. Dizaj and M. Rezvani, "The investigation of optical and mechanical properties of Er3+ doped Ga-As-S glasses quenched in different medias," *Infrared Phys. Technol.*, vol. 93, pp. 199–204, Sep. 2018, doi: 10.1016/j.infrared.2018.06.021.

[33] J. Melsheimer and D. Ziegler, “Band gap energy and Urbach tail studies of amorphous, partially crystalline and polycrystalline tin dioxide,” *Thin Solid Films*, vol. 129, no. 1, pp. 35–47, Jul. 1985, doi: 10.1016/0040-6090(85)90092-6.
[34] S. J. Ikhmayies and R. N. Ahmad-Bitar, “A study of the optical bandgap energy and Urbach tail of spray-deposited CdS:In thin films,” *J. Mater. Res. Technol.*, vol. 2, no. 3, pp. 221–227, Jul. 2013, doi: 10.1016/j.jmrt.2013.02.012.
[35] K. A. Aly, A. M. Abd Elnaeim, M. A. M. Uosif, and O. Abdel-Rahim, “Optical properties of Ge–As–Te thin films,” *Phys. B Condens. Matter*, vol. 406, no. 22, pp. 4227–4232, Nov. 2011, doi: 10.1016/j.physb.2011.08.013.
[36] K. Boubaker, “Preludes to the Lattice Compatibility Theory LCT: Urbach Tailing Controversial Behavior in Some Nanocompounds,” *ISRN Nanomaterials*, Sep. 29, 2012. https://www.hindawi.com/journals/isrn/2012/173198/ (accessed Feb. 28, 2021).